

RESEARCH ARTICLE

Comparison of CD and CDC Technologies for Flex Grid DWDM Networks

STANISŁAW KOZDROWSKI¹, PAWEŁ KRYSZTOFIK¹,
AND SŁAWOMIR SUJECKI^{2,3}, (Senior Member, IEEE)

¹Computer Science Institute, Warsaw University of Technology, 00-665 Warsaw, Poland

²Telecommunications and Teleinformatics Department, Wrocław University of Science and Technology, 50-370 Wrocław, Poland

³Faculty of Electronics, Military University of Technology, 00-908 Warsaw, Poland

Corresponding author: Stanisław Kozdrowski (stanislaw.kozdrowski@pw.edu.pl)

ABSTRACT The main objective of the paper is to compare CD and CDC nodal architecture technologies for flex grid DWDM optical networks. The methodology adopted consists in optimising a DWDM network for both nodal architectures and comparing the resource utilisation. Several nature-inspired heuristic algorithms, based mainly on an evolutionary algorithm, have been specifically selected to solve the optimisation problem with realistic computational resources. Numerical experiments were carried out for two distinct backbone networks: Polish and American. Using the best of the proposed heuristic methods in terms of the value of the objective function and computation time, CD and CDC technologies were compared. The results obtained show the advantages of CDC technology over CD technology, particularly with respect to utilization of occupied frequency bandwidth of network edges.

INDEX TERMS Metaheuristics, evolutionary algorithm, bees algorithm, mixed integer linear programming, combinatorial optimization, new-generation optical network design, DWDM, CD, CDC.

I. INTRODUCTION

Reconfigurable optical add/drop multiplexers (ROADMs) are crucial for dense wavelength division multiplexing (DWDM) networks because they support dynamic photonic layer switching without manual intervention and optoelectronic conversion [1], [2]. Next-generation ROADM enables colorless, directionless, and contentionless (CDC) wavelength routing via DWDM network nodes. Colorless attribute means that the add/drop port in ROADM is wavelength non-selective, so any wavelength can be added/dropped on any ROADM add/drop port. A colorless transponder contains a pair of transmitters and receivers for add/drop traffic without color restriction. Directionless attribute means that each ROADM add/drop port is not direction selective, so any channel added on the add/drop port can be directed to any connected node. Contentionless attribute means that the same wavelength can be added/dropped at a node provided that it relates to traffic coming from a different direction.

Nodes with only the colorless feature are limited by fixed wavelength assignments to ports and fixed direction

The associate editor coordinating the review of this manuscript and approving it for publication was Tianhua Xu ^{id}.

assignments for multiplexers. They can, therefore, only add/drop wavelengths to a fixed outgoing direction. Consequently, colorless technology introduces only limited compatibility with the concept of software-defined networking (SDN). On the other hand, the colorless architecture based on Wavelength Selective Switches (WSS) allows simple addition, dropping, and express traffic routing through network nodes and thus offers benefits such as simple planning, simple and robust capacity utilization, and low network maintenance costs. However, increasing traffic in optical networks is making C-ROADM technology increasingly obsolete due to low routing flexibility and limited adaptability to the SDN paradigm.

Colorless ROADM node architectures can remotely assign any wavelength to a specific port on a multiplexer and thus provide means to build ROADMs that automate the assignment of add/drop wavelengths. Additionally, by having colorless functionality, different wavelengths can be used for different sections of the optical path to avoid network congestion. Directionless ROADMs, on the other hand, allow any wavelength to be routed in any direction supported by the node using software control. A typical way of improving functionality of a C-ROADM is by adding directionless

attribute. The colorless and directionless (CD) ROADM modules combine the advantages of both technologies [3], [4], [5]. Fig. 1 shows a schematic diagram of a CD ROADM. A CD ROADM is constructed by combining two $1 \times$ WSSs together at the add/drop side, which removes the directional constraint of each add/drop port. However, the CD ROADM does not allow two lightpaths using the same wavelength to be added/dropped at a node.

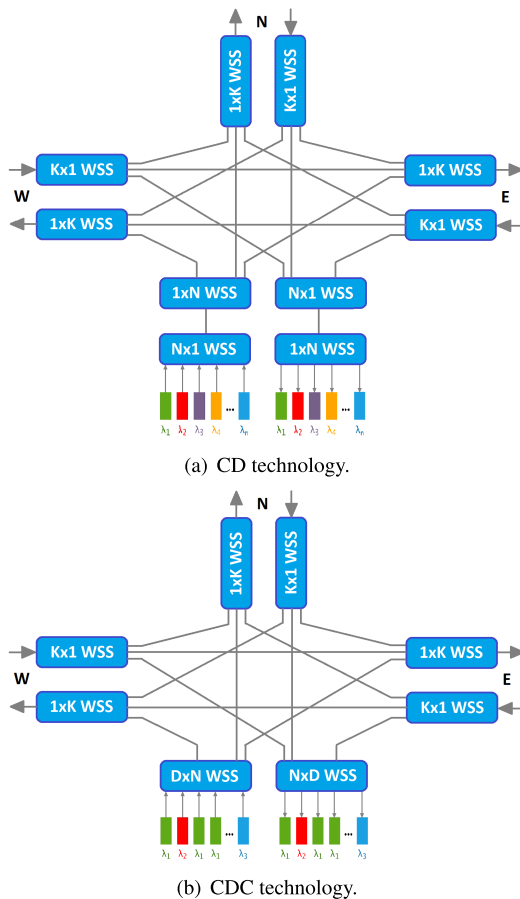


FIGURE 1. Comparison between CD and CDC technology.

Only a contentionless architecture allows multiple copies of the same wavelength on a single add/drop mux. Consequently, only a colorless, directionless architecture combined with contentionless (CDC) functionality allows exploiting fully all the bandwidth available in the transmission fibers and thus is the ultimate goal of any network operator that has implemented or plans to implement the highest level of flexibility in the optical layer [6], especially when combined with flexible wavelength assignment [7], [8]. Furthermore, the advantages of CDC technology enable operators to offer flexible services and provide significant savings in operating expenditure (OpEx) and capital expenditure (CapEx). Operational cost reductions are mainly provided by contactless provisioning and activating network capacity. Finally, it should be noted that in the case of CDC technology, the risk due to human error is greatly reduced

with fully automated provisioning [9], [10], [11]. Fig. 1(b) shows a schematic diagram of a CDC ROADM. A CDC ROADM uses $M \times N$ WSS on the add/drop side, which is a pool of add/drop ports shared by all node stages and thus overcomes the problem of wavelength contention at add/drop ports. However, since it is more difficult and expensive to produce $M \times N$ WSS than $1 \times N$ WSS, CDC ROADM is more expensive than CD ROADM.

The article aims to help telecom operators in planning the upgrade of optical networks from CD to CDC technology. In literature, there are studies available of DWDM networks with reconfigurable optical add-drop multiplexers (ROADM) [2], [12], [13]. More relevant to this contribution, studies of CD/CDC technology performed so far indicate that the CDC ROADM outperforms its non-CDC counterparts due to its wider freedom of transponder resource allocation [14], [15]. In order to further explore this topic due to its importance for optical network operators, here we perform a more detailed comparison based on numerical simulation of DWDM network performance. Particularly, this study examines the performance of a DWDM network as a function of its network size, mainly the number of nodes in the network and its node degree. The methodology adopted is based on a DWDM network optimisation subject to given demand matrix and constraints imposed by network topology. Once the optimal solution is found for CD and CDC technology separately both solutions are compared in terms of efficiency of the DWDM network resources utilisation.

Thus, the specific task considered in this paper consists in optimization of multiple DWDM networks. The optimisation problem is formulated as an integer programming (IP) problem and solved using available general-purpose solvers [16]. However, our IP optimization results show that even if the IP approach is applicable, it is inefficient for larger DWDM networks because the design task is, in general, NP-complete [17]. Numerical efficiency constraints are particularly acute in the context of routing and wavelength assignment (RWA) problems [6], [8], [18] and routing and spectrum assignment (RSA) problems [19], [20], [21], [22], which are at the heart of DWDM network optimization. Moreover, the constraints and cost functions related to a DWDM network optimisation are non-linear in the general case, and hence further complicate the numerical solution of the problem. Consequently, here we explore heuristic discrete optimization methods and apply them to optimize DWDM networks with realistic sizes and high modularity of node resources while taking into account the numerous impairments of the optical network, such as attenuation or optical signal-to-noise ratio (OSNR) [23], [24].

In summary, this paper makes two original contributions. One compares CD and CDC ROADM routing by comparing the resource utilization of both technologies. Comparison is performed by applying optimization results that minimize the network resource utilization for both technologies. Applying this methodology to DWDM networks with realistic sizes using standard optimization methods results in prohibitively

long computation times. Therefore, several heuristic methods have been proposed, and their properties are studied, which is the second contribution of this work.

This paper is organized as follows. In Section II, the problem is formulated, and the network models are described. Section III presents a description of the algorithms used in the optimization process and compares the two node technologies. Next, in Section IV, a testbed of four network structures is presented, and results of a series of numerical experiments testing the algorithms are provided and compared. Finally, Section V provides a summary of the research findings.

II. PROBLEM

In this section, we present the formulation of the optimization problem, which forms the backbone of the performed study. We formulate the optimization problem for two variations of the ROADM, namely CD ROADM and CDC one, as described in the previous section. Since CDC technology is typically offered by equipment providers together with the flex-grid technology rather than the fixed-grid one, we focus on the former variant only. Thus, in the next subsection, we give a short description of the flex-grid technology, followed by a description of the optimization model used throughout this paper.

A. FIXED-GRID AND FLEX-GRID TECHNOLOGY

CDC-ROADM technology is typically used in combination with flex-grid technology, which allows flexible bandwidth allocation across the network [25], [26]. Standard fixed-grid technology uses channels with a constant width of 50 GHz. However, as DWDM technology has developed, a need emerged to transmit signals with speeds as high as 1 Tbps, which do not fit into a single 50 GHz channel. Further, using transponders with small data rates, e.g. 10 Gbit/s with fixed grid technology, results in wasting large amounts of bandwidth as illustrated in Fig. 2.

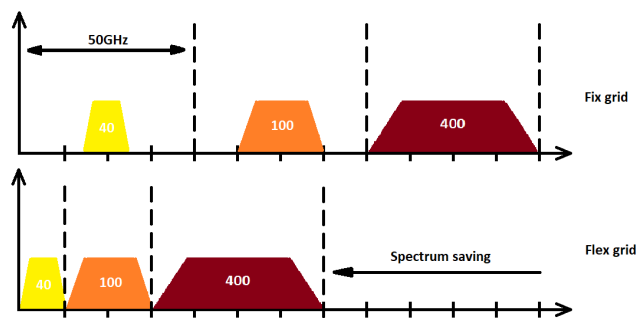


FIGURE 2. Comparison of the spectrum used by 10, 40, and 100 Gbps transponders in Fixed and Flex grid technology.

On the other hand, flexible-grid technology relies on the ability to subdivide the spectrum into arbitrary slices that are multiples of 12,5 GHz. This allows for much more efficient use of the available spectrum, as shown in Fig. 2. By comparing fix and flex grid pictures, it can be seen that with the fixed grid technology, for all digital channels, the

same bandwidth is reserved irrespective of the data bit rate. This means that a significant amount of bandwidth is wasted in the case of narrow-spectrum signals marked in green. The flex-grid technology offers, by comparison, improved spectral efficiency, which also translates into improved network ability to handle the traffic, thus making congestion less likely.

B. OPTIMIZATION MODEL

A DWDM optical network can be modeled by an undirected graph with vertices representing the individual cities and edges as the optical fibers connecting them. The main task of the network is to enable data transmission between all pairs of cities with an expected minimum throughput. The problem at hand is to solve the task of deploying enough devices in nodes of the network while minimizing their cost.

This task can be described using mathematical equations derived from [22]. It has been written as a linear optimization problem. The introduction of the model requires the definition of the following sets:

- \mathcal{N} - the set of nodes,
- \mathcal{E} - the set of edges,
- \mathcal{T} - the set of transponders,
- \mathcal{B} - the set of all bands,
- \mathcal{S} - the set of frequency slices,
- $\mathcal{P}_{(n,n')}$ - the set of all paths between nodes $n, n' \in \mathcal{N}$; $p \subseteq \mathcal{E}$,
- \mathcal{S}_b - the set of all frequency slices belonging to the band $b \in \mathcal{B}$; $\mathcal{S}_b \subseteq \mathcal{S}$; $\bigcup_{b \in \mathcal{B}} \mathcal{S}_b = \mathcal{S}$,
- \mathcal{S}_t - the set of all frequency slices that can be used as starting frequencies for transponders $t \in \mathcal{T}$; $\mathcal{S}_t \subseteq \mathcal{S}$.

Two binary decision variables are distinguished in the problem. The first is $x_{tnn'ps}$, which is the decision to install a transponder t between nodes n and n' on a path p starting from a frequency slice s . Transponders are installed only at the start and end nodes of the p path. The second y_{be} takes the value one if the bandwidth b is used on edge e and 0 otherwise.

The objective of the optimization problem is to minimize the total cost of data transmission, consisting of transponder installation and bandwidth usage, which is represented in the equation (1). The symbol $\xi(b)$ expresses the cost of using bandwidth b on a single edge (this includes, among other things, the cost of amplifiers), and $\xi(t, b)$ the cost of installing a transponder t in band b .

$$\sum_{b \in \mathcal{B}} (\xi(b) \sum_{e \in \mathcal{E}} y_{be} + \sum_{t \in \mathcal{T}} \xi(t, b) \sum_{n, n' \in \mathcal{N}} \sum_{p \in \mathcal{P}_{(n,n')}} \sum_{s \in \mathcal{S}_t} x_{tnn'ps}) \quad (1)$$

The value of the communication channel capacity demand that minimally needs to be provided between each pair of cities is defined. For a n -node network, $\frac{n(n-1)}{2}$ such demands are defined. The equation (2) shows a constraint describing this condition. The symbol $v(t)$ denotes the bandwidth a transponder guarantees t , and $\delta(n, n')$ represents the data

transmission demand between nodes n and n' .

$$\sum_{t \in \mathcal{T}} \sum_{p \in \mathcal{P}_{(n,n')}} \sum_{s \in \mathcal{S}_t} v(t) x_{tmn'ps} \geq \delta(n, n') \quad \forall n, n' \in \mathcal{N} \quad (2)$$

The mathematical model also considers some limitations due to physical phenomena occurring in optical fiber. One of these is the increasing signal degradation due to distance travel. This is related to the level of attenuation in the glass, which depends on the frequency of the light wave. On leaving the node, the signal has a certain level of power, but with distance, it loses this and becomes noisy. To prevent complete signal degradation, amplifiers are installed every second distance, usually every 60 - 100 km.

The constraint in the equation (3) ensures that the initial power of the signals coming out of the transponders is sufficient to transmit the data in the paths used. Planck's constant has been denoted by h , $v(b)$ represents the frequency of the b band, $c(t)$ is the signal-to-noise ratio of the t transponder, which has been calculated using the standard equations described in [24] among others, $\Phi(t)$ determines the bandwidth needed by the t transponder. The constant $w(n, n', p, e')$ is one if the edge e' is used on the path p between vertices n and n' . The constant $\alpha(e')$ determines how many Intermediate Line Amplifier (ILA) enhancers are installed on edge e' , which is calculated based on the edge's length. The $\pi(s)$ represents the signal power drop per kilometer for the portion of the band starting at s , and $l(e')$ is the length of the edge e' . The constants V and W define the maximum gain of the ILA. P_0 represents the transmitter output power for a single channel of the DWDM network.

$$\begin{aligned} & x_{tmn'ps} h v(b) c(t) \Phi(t) \sum_{e' \in \mathcal{E}} w(n, n', p, e') (\alpha(e') \cdot \\ & \cdot (e^{\frac{\pi(s)l(e')}{1+\alpha(e')}} + V) + (e^{\frac{\pi(s)l(e')}{1+\alpha(e')}} + W)) \leq P_0 \\ & \forall t \in \mathcal{T}, \forall n, n' \in \mathcal{N}, \forall p \in \mathcal{P}_{(n,n')}, \forall b \in \mathcal{B}, \forall s \in \mathcal{S}_b \quad (3) \end{aligned}$$

It is worth noting that the left-hand side of the equation outside the variable $x_{tmn'ps}$ can be calculated in advance and replaced by a four-dimensional parameter.

MUX/DMUX filters combine transponders' signals at a given node into one composite signal. Each of the components must have a unique frequency. It is worth noting that individual transponders may require more than one slice of frequency. For a given connection, the entire required frequency range on all edges belonging to the path used is reserved. This requirement uses the formula (4). The binary constant $u(t, s, s')$ has a value of 1 if the transponder t is installed on a slice of bandwidth starting at s and uses a slice of s' .

$$\begin{aligned} & \sum_{t \in \mathcal{T}} \sum_{n, n' \in \mathcal{N}} \sum_{p \in \mathcal{P}_{(n,n')}} \sum_{s \in \mathcal{S}_t} w(n, n', p, e) \cdot \\ & \cdot u(t, s, s') x_{tmn'ps} \leq y_{be} \\ & \forall e \in \mathcal{E}, \forall b \in \mathcal{B}, \forall s \in \mathcal{S}_b \quad (4) \end{aligned}$$

The equation (4) is also used to ensure that ILA amplifiers are installed on the bands and edges used. In principle, a constant of 1 could be placed on the right-hand side of the equation to ensure the uniqueness of the allocated frequency fragments. Using the variable y_{be} , the used edges and bands are identified, and the cost of installing the amplifiers can be simply taken into account in equation (1).

One element of the work is comparing the two types of technologies used in DWDM networks. CD technology prevents using the same frequency fragments at the node level, unlike the restriction, where the frequencies allocated at a node could be repeated if used at different edges. Another difference is that the restriction for CD technology only affects the frequencies used by the transponders allocated at the end nodes. If a signal of a given frequency does not start or end at a node but only flows through it, the constraint does not consider it. The constraint associated with CD technology was written with the formula (5).

$$\begin{aligned} & \sum_{t \in \mathcal{T}} \sum_{n' \in \mathcal{N}} \sum_{p \in \mathcal{P}_{(n,n')}} \sum_{s' \in \mathcal{S}} (x_{tmn'ps'} u(t, s, s') + \\ & + x_{m'nps'} u(t, s, s')) \leq 1 \\ & \forall n \in \mathcal{N}, \forall s \in \mathcal{S} \quad (5) \end{aligned}$$

The construction of the equation had to consider that a given transponder may occupy more than one slice of frequency. The presence of the two variables $x_{tmn'ps'}$ and $x_{m'nps'}$ on the left-hand side of the equation 5 is due to the assumption that the demand between a pair of cities is expressed only once in the constant $\delta(n, n')$ and that $\delta(n', n)$ takes the value 0. Transponders are installed at the ends of the link, so both orders should be checked. The constraint described in equation 5 applies only to CD technology. The other constraints apply to both CD and CDC nodes.

Finally, we note that the presented model does not include the limitations incurred by the four-wave mixing process. Only the effects of the amplified spontaneous emission on the OSNR are included. This allows the allocation of channels by the model, which in practice may not have a sufficiently high signal-to-noise ratio (due to four-wave mixing). As for a given network, the four-wave mixing problem becomes more acute with increasing utilization of the available bandwidth in a fiber. We believe that not including the four-wave mixing phenomenon will tip the analysis results toward predicting CDC architecture as more advantageous when compared with the CD one. Hence, we conclude that our results show the best possible performance of CDC technology when compared with CD one. The inclusion of four-wave mixing is expected to reduce the predicted benefits.

III. ALGORITHMS

The following section describes the algorithms used to solve the considered problem. We decided to use the μ , λ , $\mu + \lambda$ and bee colony algorithms. Their effectiveness was compared with the exact method (MIP) and the random method (RW).

A. $(\mu + \lambda)$ AND (μ, λ) ALGORITHMS

A $(\mu + \lambda)$ algorithm is an evolutionary algorithm used to find the optimal or sufficient solution relative to the objective function. It is initiated with an initial population of randomly created μ individuals. This initial population creates a λ of new solutions. Generation of offspring involves randomly selecting two parents from the population and mixing their parameters. For each newly generated solution, there is a small probability of a mutation occurring involving a random modification of one of the parameters. From the parent population and the generated offspring population, μ individuals are selected to form the new parent population. Individuals with a better value of the objective function are more likely to be selected. The algorithm creates new populations until one of the stopping conditions is met - usually finding a good enough solution or performing a certain number of iterations. The operation of the $\mu + \lambda$ algorithm is shown in the Algorithm 1 pseudocode.

Algorithm 1 Algorithm $\mu + \lambda$

Input: μ, λ

- 1: $P \leftarrow \text{RandomInitialization}(\mu)$
- 2: Evaluate(P)
- 3: $best \leftarrow \text{ReturnBest}(P)$
- 4: **while** stop condition is not met **do**
- 5: $P' \leftarrow \text{GenerateOffsprings}(P, \lambda)$
- 6: Evaluate(P')
- 7: $P \leftarrow \text{SelectNewPopulation}(P \cup P', \mu)$
- 8: $best \leftarrow \text{ReturnBest}(P \cup best)$
- 9: **end while**
- 10: **return** $best$

A (μ, λ) algorithm works on the same principle as the $(\mu + \lambda)$ algorithm, with the difference that only individuals from the offspring population are selected for the new parent population. The selection pressure in the algorithm depends on two factors, i.e., the way the parents interbreed and the method used for selecting individuals from the new population. When generating an offspring, the parent with the higher objective function value can be favored by increasing the probability that its parameters will be passed on to the created individual. When selecting solutions for a new population, selection pressure is influenced by how strongly we favor the selection of the better individuals. The pressure is lowest when the selection is random and highest when only the best individuals are selected. Larger selection pressure helps the algorithm to find a better solution in a shorter time but also increases the risk of stopping at a local maximum. This may occur when all population members are close to each other in the state space. The newly created solutions, even after mutation, will not be significantly different from their parents and will, therefore, have a similar objective function value. Such a situation would, in consequence, prevent the algorithm from finding

a solution with a significantly better value of the objective function.

B. BEE COLONY ALGORITHM

An alternative to the $(\mu + \lambda)$ algorithm is the Bee Colony (BC) algorithm. Compared to the $(\mu + \lambda)$ algorithm, BC searches a larger region of the state space and has an in-built mechanism to prevent it from stopping at a local maximum. BC is based on an initially randomly generated population of N individuals. During each iteration, new individuals are generated in three ways.

- 1) The m best individuals are selected from the population. Each selected individual can be drawn as a parent for a new offspring. A new solution is created based on a single parent. In this case, the new solution has the same parameters as the parent, except for some that are subjected to the mutation operator. By randomly selecting parents, $m - e$ new solutions are created;
- 2) From a population of m individuals, e of those with the best value of the objective function is selected. For each selected individual k offspring solutions are created;
- 3) $N - m$ new individuals are randomly generated.

By generating new, entirely random individuals, the algorithm can find a better solution than the one it encountered in the local minimum. Selection pressure will be determined by the selection methods and the parameters m , e , and k . Decreasing the parameters m and e and increasing the parameter k will increase the selection pressure. The operation of the BC algorithm is shown in the Algorithm 2 pseudocode.

Algorithm 2 Bee Colony Algorithm

Input: N, m, e, k

- 1: $P \leftarrow \text{RandomInitialization}(N)$
- 2: Evaluate(P)
- 3: $best \leftarrow \text{ReturnBest}(P)$
- 4: **while** stop condition is not met **do**
- 5: $bestBees \leftarrow \text{SelectBest}(P, m)$
- 6: $eliteBees \leftarrow \text{SelectBest}(bestBees, e)$
- 7: $bestSol \leftarrow \text{RandomNeighbors}(bestBees, m - e)$
- 8: $eliteSol \leftarrow \text{EliteNeighbors}(eliteBees, k)$
- 9: $randomSol \leftarrow \text{RandomNeighbors}(P, \text{Max}(N - m, m - N))$
- 10: $P \leftarrow \text{SelectNewPopulation}(P \cup bestSol \cup eliteSol \cup randomSol, N)$
- 11: $best \leftarrow \text{ReturnBest}(P \cup best)$
- 12: **end while**
- 13: **return** $best$

C. RANDOM WALK ALGORITHM

A random walk (RW) algorithm involves randomly creating new individuals. The algorithm keeps only the best solution in memory. In each iteration, one individual is created, and if it has a better value of the objective function than the stored

solution, it takes its place. There is no selection pressure in the algorithm.

In theory, it may find the best possible solution, but the probability of this is low in practice. The algorithm compares the effectiveness of heuristics against random solution generation. The operation of the RW algorithm is shown in the Algorithm 3 pseudocode.

Algorithm 3 Random Walk Algorithm

```

1:  $best \leftarrow CreateRandomSolution()$ 
2: Evaluate( $best$ )
3: while stop condition is not met do
4:    $newSolution \leftarrow CreateRandomSolution()$ 
5:   if  $newSolution.goalFunctionValue <$ 
      $best.goalFunctionValue$  then
6:      $best \leftarrow newSolution$ 
7:   end if
8: end while
9: return  $best$ 

```

D. MIXED INTEGER PROGRAMMING

In short, the mixed integer programming (MIP) algorithm contains the following steps.

- Formulate a model, the abstract system of variables, objectives, and constraints representing the general form of the problem to be solved.
- Collect data that define a specific problem instance.
- According to the model analyzed and the data for this model, generate an appropriate objective function and set of constraints.
- Solve the problem instance by running a solver to apply an algorithm that finds optimal values of the variables.
- Analyze the results.
- Refine the model and data as necessary and repeat.

The CPLEX optimization software package [27] was used to implement MIP with constraints, which applies the branch-and-bound method to solve MIP problems. MIP consists of searching a tree representing the solution space of a problem using branching and bounding procedures. Branching consists of performing splitting and creating disjoint subtrees from a given node. The bounding procedure reduces the number of explored nodes by skipping a branch when it is known that this branch does not contain an optimal solution in its leaves [28].

The mathematical model describing the problem was implemented in the AMPL language. This language is dedicated to modeling mathematical problems, whose syntax resembles the algebraic notation [29]. The AMPL system converts the model file and parameter value file into a form that is readable by the optimizer. The problem model contains the definition of decision variables, objective functions, constraints, and the declaration of the model sets and parameters. The values of the sets and parameters are transferred in a DAT file. The processed file is then passed

to the CPLEX optimization engine. The algorithm runs until it finds the optimal solution to the problem. However, for the NP-complete problems considered in this work, it is necessary to provide a stop criterion as a maximum running time, e.g., 10^6 seconds.

IV. RESULTS

The description of the results is divided into four subsections. First, the method for generating the network topologies used for testing is presented in subsection IV-A. Then, the model parameters are discussed in IV-B. The third subsection IV-C compares the proposed algorithms in terms of the value of the objective function and computational complexity. The last subsection IV-D deals with a detailed comparison of CD and CDC technologies for selected test networks.

A. NETWORK TOPOLOGIES

The relative advantages of CD and CDC technology have been compared for artificially generated optical networks based on the Polish and American backbone networks. Both considered networks differ in the number of nodes and the degree of each node. The number of nodes considered for both networks equals 3, 5, 10, and 15. The cities, which correspond to the specific nodes, were taken from files from the SNDlib database [30]. Thus, an additional three cities had to be added to create the 15-node Polish network, which in SNDlib consists only of 12 nodes. These additional cities were selected from the list of the most populated Polish cities according to the data published by the Polish Statistical Office in 2020. The American backbone network consists of 26 nodes, so there was no need to add cities since the largest considered network has 15 nodes. Table 1 shows the Polish and American cities selected for the experiments.

TABLE 1. Polish and American cities selected for network generation for a given value of a number of nodes.

# nodes	Polish cities	American cities
3	Łódź, Katowice, Wrocław	Seattle, Chicago, N.Y.
5	Łódź, Katowice, Wrocław Warszawa, Kraków	Seattle, Chicago, N.Y. Houston, L.A.,
10	Łódź, Katowice, Wrocław War., Kr., Poznań, Białystok Bydgoszcz, Gdańsk, Szczecin	Seattle, Chicago, N.Y., L.A. Houston, Atlanta, Dallas Denver, Miami, W.D.C
15	Łódź, Katowice, Wrocław War., Kr., Poznań, Białystok Bydgoszcz, Gdańsk, Szczecin Olsztyn, Kołobrzeg, Kielce Lublin, Rzeszów	Seattle, Chicago, N.Y., L.A. Houston, Atlanta, Dallas Denver, Miami, W.D.C Minneapolis, Kansas City Las Vegas, Detroit, Houston

Thus, configuration files were created, which contain a list of fifteen cities taken from files in the SNDlib database, including three additional cities in the case of the Polish network. For 3-node networks, the node degree can be only one ($n_d = 2$); for 5-node networks the node degree is determined by the set: $n_d \in \{2, 3, 4\}$, while for 10-node and 15-node networks the set of numbers that determine the node degree is as follows: $n_d \in \{2, 3, 4, 5, 6\}$.

The problem of generating a graph in which the nodes have a given number of degrees is well-known in the literature. One of the first algorithms invented to solve this problem is the Havel-Hakimi algorithm [31]. This algorithm generates the desired network sequentially.

The second algorithm often used in practice is described in [32]. It is used to find a random network satisfying the node degree condition. In contrast to the Havel-Hakimi algorithm, this other algorithm iterates over edges. In each step, two vertices are drawn with a probability proportional to the product of the number of edges still to be connected to them. These algorithms inspired the edge generation method for the networks analyzed. The details are contained in Algorithm 4.

Algorithm 4 Edge Generation

Input: $nodes_0$, $edges_0$, $degree$, $max_restart$

```

1:  $i \leftarrow 0$ 
2: while  $i < max\_restart$  do
3:    $nodes \leftarrow nodes_0$ 
4:    $edges \leftarrow edges_0$ 
5:   while True do
6:     if isFinished( $nodes$ ,  $degree$ ) then
7:       return  $nodes$ ,  $edges$ 
8:     end if
9:      $source \leftarrow$  selectFirstNode( $nodes$ )
10:     $targets \leftarrow$  filterPossible( $nodes$ ,  $source$ ,  $degree$ )
11:    if isEmpty( $targets$ ) then
12:      break
13:    else
14:       $target \leftarrow$  getClosest( $source$ ,  $targets$ )
15:       $nodes$ ,  $edges \leftarrow$  update( $source$ ,  $target$ ,  $nodes$ ,  $edges$ )
16:    end if
17:  end while
18:   $i \leftarrow i + 1$ 
19: end while
20: return error

```

The input parameters are the current network passed as collections of nodes ($nodes_0$) and edges ($edges_0$), as well as the target degree of nodes ($degree$) and the maximum number of iterations allowed ($max_restart$). The designed function in consecutive iterations appends one edge at a time to the existing network until all nodes have reached the desired degree (**isFinished**). The initial node is drawn randomly from the list of all nodes with the smallest current degree (**selectFirstNode**). The remaining nodes are filtered, selecting those missing an edge and no longer connected to the node (**filterPossible**). If no possible connections are found, another attempt to add edges is started from the network state passed in the input argument. Otherwise, from the filtered nodes, the nearest neighbor of the starting node is selected (**getClosest**), and the network state is updated with the added edge (**update**).

The method described in the Algorithm 4 is simple but entirely sufficient to generate the requested graphs. The algorithm is greedy, and the decision is made to add an edge for the node missing the most in a given iteration and connect it to its nearest possible neighbor. Finally, according to the description, the following networks were generated for testing:

- 1) for the Polish network (Fig. 3(a) – 3(d)) there are 3-node, 5-node, 10-node, and 15-node networks with the highest possible node degree n_d (2 – for the 3-node network, 4 – for the 5-node network and 6 for the 10- and 15-node network);
- 2) for the American network (Fig. 4(a) – 4(d)) there are 3-node, 5-node, 10-node, and 15-node networks with the same node degree n_d as in the case of the Polish network.

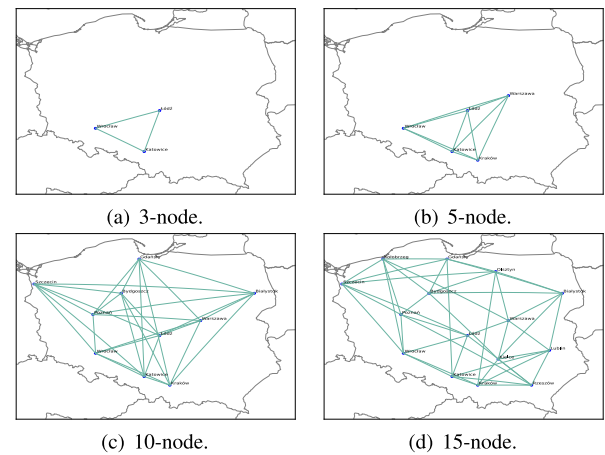


FIGURE 3. Polish networks topology used in numerical experiments.

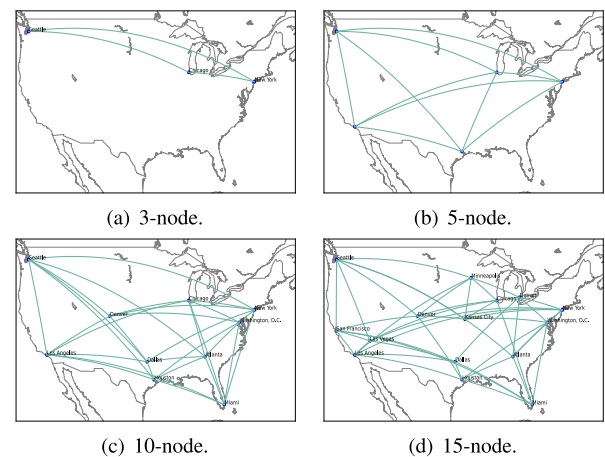


FIGURE 4. American networks topology used in numerical experiments.

B. MODEL PARAMETER DESCRIPTION

The calculations were carried out for specific and typical practical applications parameter values of the model, described in Section II. All experiments were performed on

next-generation DWDM networks using flex-grid technology. Network parameters are identical to those in Table 2.

TABLE 2. Network parameter values used in numerical experiments.

Symbol	Description	Example values
\mathcal{N}	# nodes for both, Polish and American networks	3, 5, 10, 15
\mathcal{E}	# links for both, Polish and American networks	3, 10, 30, 45
\mathcal{D}	# demands for both, Polish and American networks	3, 10, 45, 105
\mathcal{B}	# band	1
\mathcal{S}	# slice frequency	384
$v(t)$ [Gbps]	transponder transmission rate	$v(t)=[10; 40; 100; 200; 400]$
$c(t)$ [dB]	transponder's OSNR	$c(t)=[10; 11; 12; 15; 22]$
$\xi(t, b)$	cost of using a transponder in the band	$\xi(t, b)=[1; 3; 5; 7; 9]$
$\xi(b)$	cost of using a band on edge	$\xi(b)=[1]$
$\Phi(t)$ [GHz]	bandwidth used by the transponder	$\Phi(t)=[12.5; 25; 50; 62.5; 87.5]$
$\nu(b)$ [THz]	frequency of the band b	$\nu(b)=193.8$
$\pi(s)$ [dB/km]	drop in signal power on a frequency slice s	$\pi(s)=0.046$

The number of nodes and edges is a test parameter. Technologies are compared for different topologies and sizes. Due to the computational complexity, each problem was assumed to have two or three predefined paths. The specific values of the simulation parameters are summarized in Table 2.

The parameter values of the algorithms are presented in tables, respectively, for the BC algorithm in Table 3 and for the AE algorithm in Table 4.

TABLE 3. Values of the bee colony parameters adopted during the benchmark tests.

Parameter	Description	Value
N	population size	50
m	number of best bees	30
I	number of iterations	100
e	number of elite bees	5
k	number of offspring per elite bee	5

TABLE 4. Values of the evolutionary algorithms adopted during the tests in both variants $(\mu+\lambda)$ and (μ,λ) .

Parameter	Description	Value
μ	size of base population	50
λ	size of the temporary iteration	50
I	number of iterations	100
p_k	probability of crossover	0.8
p_m	probability of mutation	0.2

The numerical simulations were conducted to analyze networks of different dimensionality. Four network cases were considered for the Polish and American networks: 3, 5, 10, and 15-node. The topologies of these networks are shown in Figs 3 and 4 for the Polish and American networks,

respectively. The calculations were done on a 3.6 GHz Intel Core processor with 16 GB RAM under the Linux Ubuntu operating system. Tables 2, 3, and 4 contains all relevant simulation parameters.

C. METAHEURISTICS COMPARISON

It is well known that as the size of the optimized network increases, the time required to find an admissible solution using the exact Mixed Integer Programming (MIP) algorithm increases. Thus, the simulation time may become prohibitively large for networks with many nodes. Therefore, we carried out simulations using selected heuristic methods described in Section III. The methodology used consisted of searching for the optimal solution using heuristic algorithms and comparing these results with the results of simulations performed using the CPLEX optimizer (MIP method). The computational time to solve the problem was used to compare the efficiency of the different methods.

Based on the results presented in Tables 5 and 6, and in Figure 5, the following observations can be made.

- All the heuristic methods reached a solution that is either optimal or close to optimal.
- The reference methods (MIP and RW) were generally inferior to heuristic methods. The RW algorithm often fails to reach the optimal solution for small and larger networks. However, the MIP method for small networks (3-nodes and 5-nodes) performed well and reached the optimal solution within a short computational time. However, the computation time was significantly longer for larger networks (10 and 15-node networks) compared to heuristic methods.
- Comparing the heuristic methods, it can be seen that in all cases, the $(\mu + \lambda)$ and (μ, λ) methods give slightly better results than the BC method. It is especially noticeable in the case of the Polish network, where the results obtained by the BC method are a few percent worse regarding both the value of the objective function and the computation time. In the case of the American network, these differences are less than one percent in favor of the evolutionary methods.
- is particularly noteworthy that the computation time for the MIP method, compared to heuristic methods, is shorter for smaller, 3-node, and 5-node networks. It is noticeable that the curves intersect at the 6, 7-node level. The situation is reversed for the larger, 10-node, and 15-node networks. For the 10-node network, the calculation time is already greater than two orders of magnitude. For the 15-node network, on the other hand, a stop criterium of time 10^6 seconds was used. However, the suboptimal solution found is close to the optimum.
- RW method only found an optimal solution for the Polish 3-node network. In the other cases, the solutions found were far from optimum.
- The computation time curves for the two networks analyzed are very similar in terms of convergence. This indicates a valuable feature of the proposed methods.

TABLE 5. Average value of the objective function and average computation time calculated by selected algorithms for Polish network. The results were obtained by averaging 20 independent runs for each algorithm except MIP, a deterministic method that was only run once for each network. *A stop criterion was applied for the 15-node networks (10^6 seconds).

Algorithm	3-node		5-node		10-node		15-node	
	fitness	time [s]	fitness	time [s]	fitness	time [s]	fitness	time [s]
$\mu + \lambda$	2010.0	60.1	6310.0	405.6	12720.0	625.2	13216.6	677.8
BC	2010.0	64.6	6893.2	446.6	16896.4	820.8	15370.9	945.3
μ, λ	2010.0	61.0	6310.0	430.8	12720.0	648.6	13221.3	688.2
RW	2010.0	180.4	369613.2	814.1	557769.8	1167.6	706994.8	1301.9
MIP	2010.0	9.2	6309.0	63.2	12720.0	155568.4	13214.0	10e6*

TABLE 6. Average value of the objective function and average computation time calculated by selected algorithms for an American network. The results were obtained by averaging 20 independent runs for each algorithm except MIP, a deterministic method that was only run once for each network. *A stop criterion was applied for the 15-node networks (10^6 seconds).

Algorithm	3-node		5-node		10-node		15-node	
	fitness	time [s]	fitness	time [s]	fitness	time [s]	fitness	time [s]
$\mu + \lambda$	2010.0	77.9	5410.0	266.8	11214.7	469.0	16642.5	776.9
BC	2010.0	85.1	5410.0	282.1	11234.7	522.5	16742.6	808.7
μ, λ	2010.0	79.5	5439.8	284.4	11214.4	471.7	16644.4	772.8
RW	6795.6	171.4	212595.8	604.9	180958.0	811.2	79159.7	1028.8
MIP	2010.0	9.4	5409.0	64.9	11215.0	159082.5	16643.0	10e6*

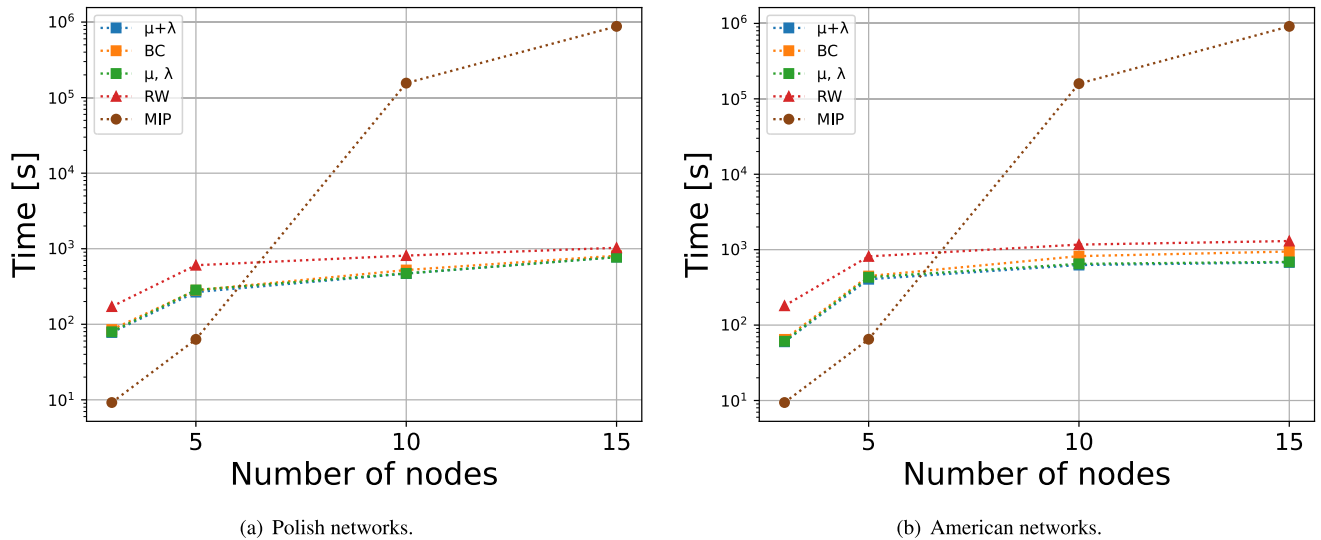


FIGURE 5. The dependence of computational time on number of nodes.

In summary, based on the results shown in Fig. 5 and Tables 5 and 6, it can be concluded that for small networks (up to 6 nodes), the MIP exact method can be used. However, heuristic methods for larger networks (more than 6 nodes) are advisable primarily because of calculation time and a satisfactory near-optimal solution.

The best heuristic method for the objective function and computation time was found to be the $\mu + \lambda$ method. Therefore, this method was used to perform numerical simulations comparing CD and CDC technologies.

D. CD AND CDC COMPARISON

The main parameter we use to compare CD and CDC technologies is bandwidth utilization in each edge of the DWDM networks considered (Polish and US). Only the

C-band was considered, and bandwidth utilization was defined as the percentage of the total available bandwidth in the C-band (384×12.5 GHz) occupied by allocated traffic. Numerical simulations compared CD and CDC technologies, considering edge traffic and frequency slice allocation. It was assumed that the demand matrix considers all possible pairs of nodes (cities) and that all elements of the demand matrix have the same value. In accordance with the conclusions of the previous subsection, the $\mu + \lambda$ algorithm was used for the cost function optimization, defined in section II.

Tables 7 and 8 show the dependence of the average bandwidth usage on the value of the demand matrix element and network node degree for Polish and American networks, respectively. The average bandwidth usage was obtained by summing values of bandwidth usage for all network

edges and dividing the sum by the number of edges. The parameter d_{max} is the maximum value of the simulation's demand matrix element. d_{max} is calculated numerically by increasing the value of the demand matrix element until the optimization algorithm fails to allocate all the demands. The highest value of the demand matrix element is the one for which the optimization algorithm succeeded in allocating all demands equal to d_{max} . Fig. 6 gives the dependence of d_{max} on node degree for each network and technology considered. Thus, to correctly interpret the results shown in Tables 7 and 8, one needs to refer to Fig. 6 to read the correct values of the maximum value of the demand matrix element - d_{max} because it varies for each row of both Tabs and each technology.

The results from Tables 7 and 8 show that for CD technology with a large node degree, the average bandwidth occupancy reaches approximately 30% at d_{max} . This indicates that with a high node degree, CD technology severely limits the use of the available bandwidth. This, in turn, has important consequences for the opex of a Network Operator (NO) since the fibers are usually rented on the price per kilometer cost basis rather than the bandwidth used.

Thus, low bandwidth usage of fibers leads to excessive opex and possibly also a non-viable business plan in the long term. This issue is further exacerbated by the fact that with the growing node degree, the value of d_{max} remains fairly constant for CD technology, as shown in Fig. 6. Therefore, if a network initially consists of low-degree nodes and then is expanded to larger-degree nodes, a NO may observe that the opex scales up very quickly. At the same time, the allocated traffic gains are very moderate. A completely different picture emerges for the CDC technology when considering the results shown in Tables 7 and 8, and Figure 6. First of all, d_{max} increases linearly with node degree (Figure 6). Further, at d_{max} , the bandwidth occupancy reaches almost

TABLE 7. Average bandwidth usage at selected values of demand matrix element for Polish network.

5-node network, bandwidth usage [%]								
node degree	0,25 d_{max}		0,5 d_{max}		0,75 d_{max}		d_{max}	
	CD	CDC	CD	CDC	CD	CDC	CD	CDC
2	29,6	35,3	49,6	68,7	63,1	93,6	59,5	98,8
3	15,4	33,6	25,6	62,5	37,5	89,0	52,1	99,4
4	9,0	32,8	15,3	60,6	22,5	77,4	31,4	91,7

10-node network, bandwidth usage [%]								
node degree	0,25 d_{max}		0,5 d_{max}		0,75 d_{max}		d_{max}	
	CD	CDC	CD	CDC	CD	CDC	CD	CDC
2	33,6	46,6	73,8	83,3	73,4	93,2	72,2	93,8
3	18,7	22,1	39,3	50,4	59,9	68,6	66,6	84,4
4	15,3	28,4	22,8	50,9	37,5	77,0	45,1	92,8
5	10,7	22,8	16,3	46,1	26,9	68,6	32,1	86,4
6	8,5	24,1	13,2	48,3	21,3	67,8	25,3	81,9

15-node network, bandwidth usage [%]								
node degree	0,25 d_{max}		0,5 d_{max}		0,75 d_{max}		d_{max}	
	CD	CDC	CD	CDC	CD	CDC	CD	CDC
2	67,9	84,4	56,2	81,9	80,2	92,2	81,6	95,0
3	31,0	30,0	39,6	38,3	42,4	43,9	52,3	51,9
4	14,0	23,3	30,6	33,0	45,0	46,8	46,5	62,7
5	11,9	21,8	23,4	33,2	27,6	53,9	36,2	63,5
6	11,2	20,0	15,1	43,6	26,2	58,1	29,8	70,5

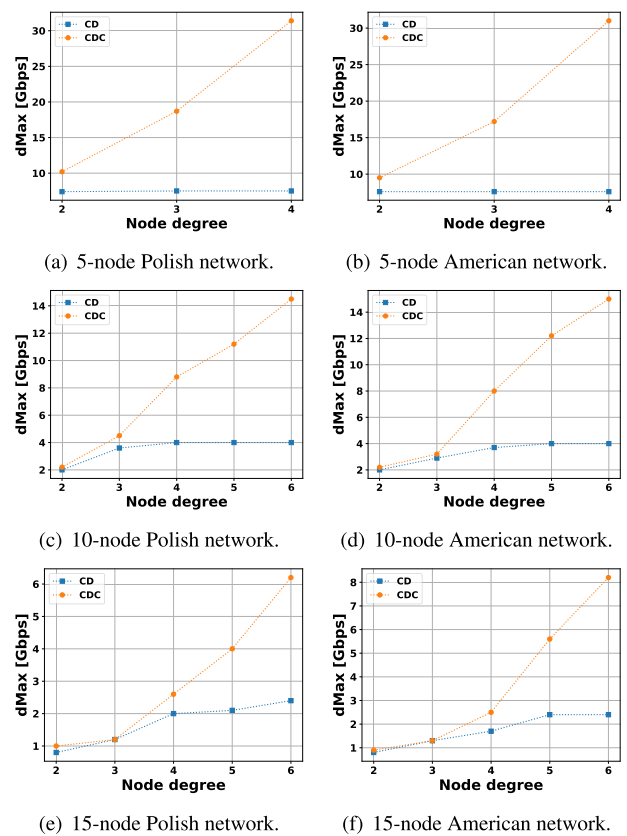


FIGURE 6. Dependence of maximum value of the demand matrix element on node degree.

consistently 90%. These results show that from a NO point of view, CDC technology allows for more flexibility with respect to network expansion planning as it allows for increasing the node degree without penalty in bandwidth usage.

TABLE 8. Average bandwidth usage at selected values of demand matrix element for American network.

5-node network, bandwidth usage [%]								
node degree	0,25 d_{max}		0,5 d_{max}		0,75 d_{max}		d_{max}	
	CD	CDC	CD	CDC	CD	CDC	CD	CDC
2	26,0	27,7	52,8	66,6	61,8	84,9	59,8	99,4
3	15,0	29,7	25,6	56,5	37,6	81,8	51,6	97,0
4	9,3	30,1	16,3	57,8	21,5	74,5	29,2	88,8

10-node network, bandwidth usage [%]								
node degree	0,25 d_{max}		0,5 d_{max}		0,75 d_{max}		d_{max}	
	CD	CDC	CD	CDC	CD	CDC	CD	CDC
2	37,1	49,1	68,0	79,8	75,8	92,6	72,2	94,9
3	15,4	15,7	35,1	31,3	47,7	51,0	59,2	59,2
4	12,8	24,0	25,7	46,6	32,4	71,1	44,1	89,5
5	10,5	26,9	16,5	50,9	26,9	73,2	32,6	92,5
6	8,6	25,9	13,0	50,2	21,1	69,2	26,2	87,0

15-node network, bandwidth usage [%]								
node degree	0,25 d_{max}		0,5 d_{max}		0,75 d_{max}		d_{max}	
	CD	CDC	CD	CDC	CD	CDC	CD	CDC
2	68,7	81,8	54,0	77,0	79,8	92,3	78,2	93,3
3	21,4	20,5	44,0	43,2	50,5	50,0	57,8	61,1
4	11,6	24,0	23,7	32,2	31,6	54,1	41,8	63,5
5	13,7	25,8	18,1	42,1	32,1	67,2	36,9	81,7
6	10,2	24,7	13,6	47,3	23,5	70,6	26,8	88,5

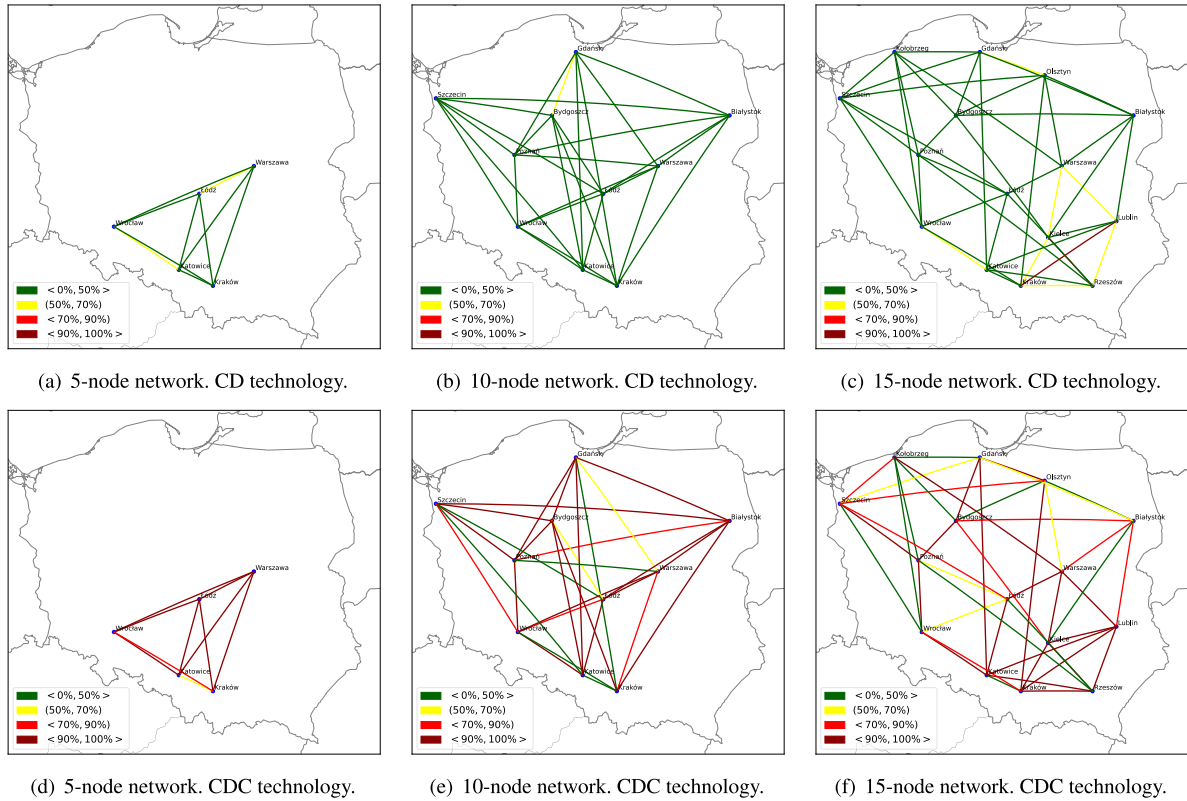


FIGURE 7. Bandwidth usage map for the polish networks analyzed.

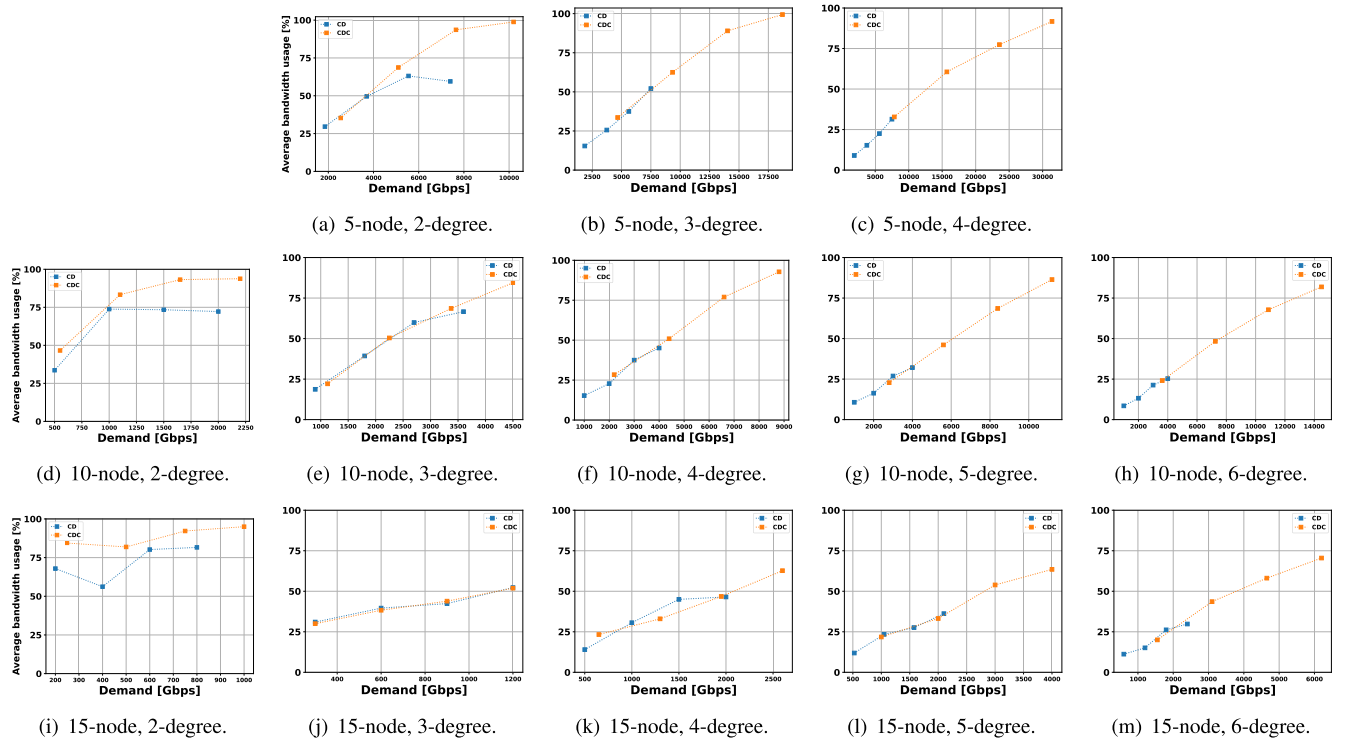


FIGURE 8. Averaged network bandwidth usage as a function of demand, for Polish network.

Contrary to previous observations, when NO plans to deploy a ring network, i.e., a network with a low node degree, then there are significantly less benefits to using CDC

technology instead of a simpler and cheaper CD technology, according to the results shown in Tables 7 and 8, and Figure 6. This rather is because both technologies offer much

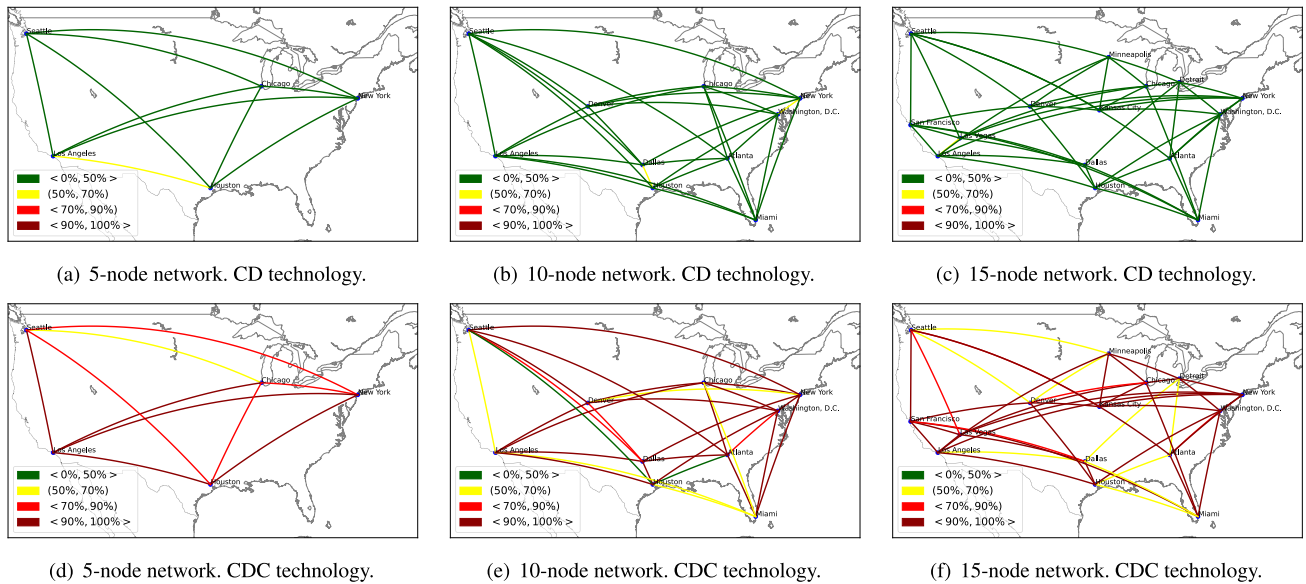


FIGURE 9. Bandwidth usage map for the American networks analyzed.

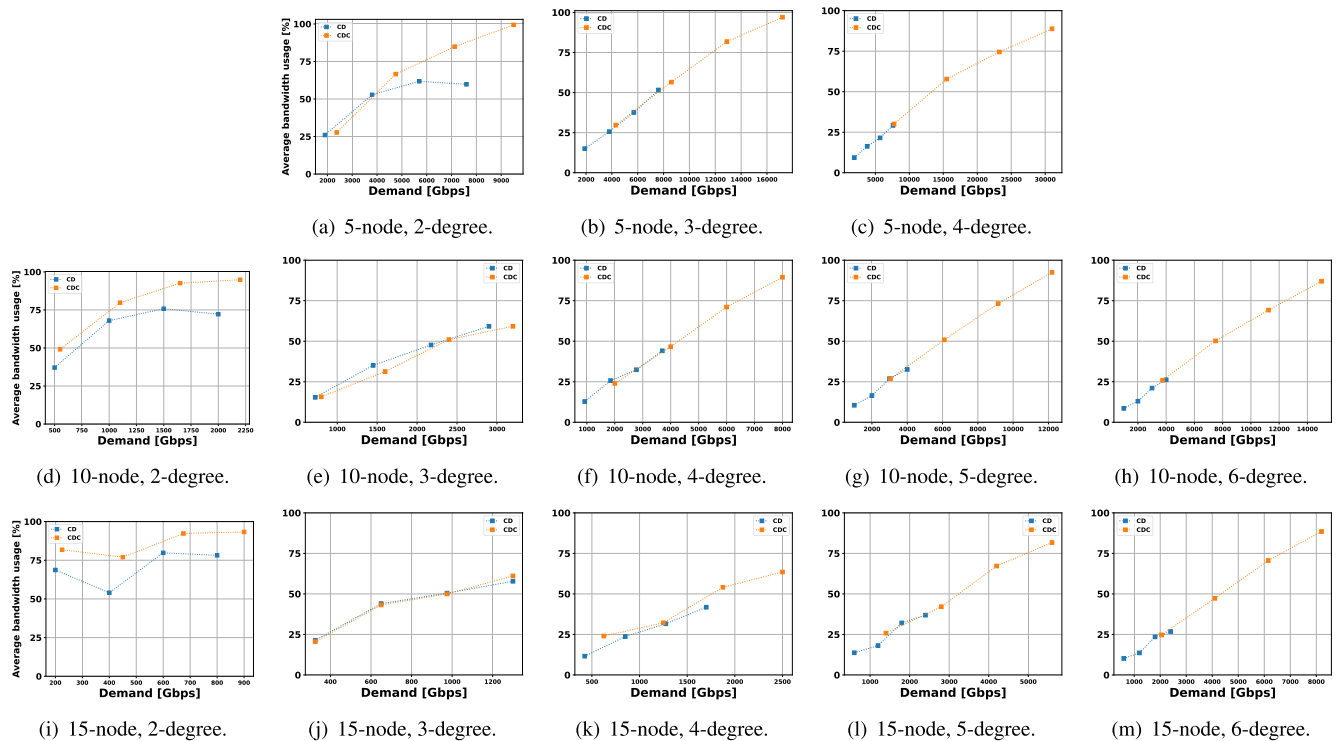


FIGURE 10. Averaged network bandwidth usage as a function of demand for American network.

more similar bandwidth usage. Interestingly, the results from Tables 7 and 8 show that the difference between CD and CDC technology decreases with the number of nodes. This is surprising because, for the ring network, one would expect that the older technology (CD) should use not more than 50% of the bandwidth on average. This is because, for each node, the allocated frequency in one edge blocks usage of the same frequency in the other network edge stemming from the same

node. This, however, applies to traffic terminated in a given node only. We will investigate this issue further in the next paragraphs.

In order to further investigate the bandwidth usage by CD and CDC technology, a map was created for the networks under study, showing the bandwidth usage of the network edges. Colors were used to indicate the level of bandwidth utilization, where green to maroon colors indicate edges with

increasing bandwidth utilization, with green corresponding to a low level of bandwidth utilization. In contrast, maroon indicates a high level of bandwidth utilization. The results obtained for the test cases are shown in Figures 7 and 9 for the Polish and US networks, respectively. These results were obtained assuming the maximum possible amount of traffic allocated for each technology, i.e., CD and CDC.

The results from Figures 7 and 10 show that in the case of CD technology, the network edges are predominantly depicted by a shade of green. Hence, the corresponding bandwidth usage level is low, mostly less than 50%, and rarely achieves levels within the interval between 50% and 80%. Thus, much of the bandwidth available in the edges is unused. Only very rarely it is possible to use more than 50% of the available bandwidth with CD technology, as confirmed by the Figures for the Polish network (7(a) – 7(c)), and for the American network (9(a) – 9(c)).

For CDC technology, the dominant colors are shades of red, which was to be expected given the higher value of realized demands for this technology. In addition, some of the edges are fully utilized, which is best seen in the networks, shown in Figures 7(d) – 7(f), for the Polish network and 9(d) – 9(f), for the American network, respectively.

To further investigate the bandwidth usage by CD and CDC technology, we have calculated the dependence of the average bandwidth usage on the value of the demand matrix element (Fig. 8 and Fig. 10). These results show that as the node degree increases, the curves for the different technologies move further apart. The demand values for CD technology change only slightly, and the adopted bandwidth occupancies do not exceed 25%. A different trend is noticeable for the CDC technology: the demands increase, and the average bandwidth occupancy is at the level of 100%. Notably, the most significant difference between CD and CDC technologies is the maximum demand value, d_{max} , which increases further with increasing node degrees in the network. This is particularly noticeable in Fig. 8(c), 8(h) and 8(m) for the Polish network and in Fig. 10(c), 10(h) and 10(m) for the American network, respectively.

This leads to the conclusion that CDC technology is recommended for operators of large telecom networks since it almost fully utilizes the available bandwidth for dense networks with a large node degree and high throughput requirements. This conclusion is essential given the current trend in the industry. Excluding exceptional cases, as demand increases for each network and both technologies, an increase in bandwidth occupancy is observed, as can be seen in the Figures 8 and 10 figures for the Polish and American networks.

V. CONCLUSION

In this paper the advantages of CD and CDC technology were studied. For this purpose, network resource allocation for both CD and CDC technology was optimized using numerical algorithms, and the bandwidth usage was compared. Numerical simulations were conducted using

selected meta-heuristics. The results obtained show that using metaheuristics rather than standard methods (e.g., Mixed Integer Programming) for network problems of practical importance is essential, especially for large networks with many nodes and edges due to insufficient computational efficiency of the standard methods. Among metaheuristics, the $(\mu + \lambda)$ method was found to be the most efficient one for optimizing the considered networks.

A CDC and CDC technology comparison was performed for a Polish and American network taken from the SNDlib library. The results show that the CDC technology outperforms CD one for both considered networks, especially when the network consists of high-degree nodes. In the case of ring networks, the benefits of using CDC technology compared to CD one are much more moderate. However, there is still a clear advantage in using CDC technology, mainly because it provides a much more flexible and open platform for a possible future network expansion.

In future work, we plan to include the effect of four-wave mixing on the path allocation process in the routing algorithm.

REFERENCES

- [1] D. Wang, M. Zuo, D. Guan, J. Gu, T. Lu, D. Ge, J. Wang, Y. Li, S. Shi, J. Sun, L. Han, D. Zhang, and H. Li, "Demonstration of a cost-effective WSS-free colorless flex-grid ROADM with coherent detection and wavelength monitoring for optical metro networks," in *Proc. Opto-Electron. Commun. Conf. (OECC)*, Jul. 2023, pp. 1–3.
- [2] M. U. Masood, I. Khan, L. Tunisi, B. Correia, E. Ghillino, P. Bardella, A. Carena, and V. Curri, "Network performance of ROADM architecture enabled by novel wideband-integrated WSS," in *Proc. GLOBECOM-IEEE Global Commun. Conf.*, Dec. 2022, pp. 2945–2950. [Online]. Available: <https://api.semanticscholar.org/CorpusID:255598730>
- [3] J. Pedro and S. Pato, "Towards fully flexible optical node architectures: Impact on blocking performance of DWDM transport networks," in *Proc. 13th Int. Conf. Transparent Opt. Netw.*, Jun. 2011, pp. 1–4.
- [4] R. Jensen, A. Lord, and N. Parsons, "Highly scalable OXC-based contentionless ROADM architecture with reduced network implementation costs," in *Proc. OFC/NFOEC*, Mar. 2012, pp. 1–3.
- [5] P. N. Ji and Y. Aono, "Colorless and directionless multi-degree reconfigurable optical add/drop multiplexers," in *Proc. 19th Annu. Wireless Opt. Commun. Conf. (WOCC)*, May 2010, pp. 1–5.
- [6] A. Cai, G. Shen, L. Peng, and M. Zukerman, "Novel node-arc model and multiiteration heuristics for static routing and spectrum assignment in elastic optical networks," *J. Lightw. Technol.*, vol. 31, no. 21, pp. 3402–3413, Nov. 2013.
- [7] S. Kozdrowski, M. Zotkiewicz, and S. Sujecki, "Resource optimization in fully flexible optical node architectures," in *Proc. 20th Int. Conf. Transparent Opt. Netw. (ICTON)*, Jul. 2018, pp. 1–4.
- [8] M. Klinkowski and K. Walkowiak, "Routing and spectrum assignment in spectrum sliced elastic optical path network," *IEEE Commun. Lett.*, vol. 15, no. 8, pp. 884–886, Aug. 2011.
- [9] Y. Li, J. Li, L. Zong, S. K. Bose, and G. Shen, "Upgrading nodes with colorless, directionless, and/or contentionless ROADMs in an optical transport network," in *Proc. 22nd Int. Conf. Transparent Opt. Netw. (ICTON)*, Jul. 2020, pp. 1–4.
- [10] C. Papapavlou, K. Paximadis, and G. Tzimas, "Analyzing ROADM costs in SDM networks," in *Proc. 11th Int. Conf. Inf., Intell., Syst. Appl. (IISA)*, Jul. 2020, pp. 1–7.
- [11] J. M. Rivas-Moscoco, B. Shariati, D. M. Marom, D. Klonidis, and I. Tomkos, "Comparison of CD(C) ROADM architectures for space division multiplexed networks," in *Proc. Opt. Fiber Commun. Conf. Exhibi. (OFC)*, Mar. 2017, pp. 1–3.
- [12] D. C. Morão, L. G. Cancela, and J. L. Rebola, "Exploring future large-scale ROADM architectures," in *Proc. Telecoms Conf. (ConfTELE)*, Feb. 2021, pp. 1–6.

- [13] J. F. Ó. Ramos, L. Cancela, and J. Rebola, "Influence of the ROADM architecture on the cost-per-bit in C+L+S multi-band optical networks," in *Proc. 23rd Int. Conf. Transparent Opt. Netw. (ICTON)*, Jul. 2023, pp. 1–4.
- [14] M. U. Masood, I. Khan, L. Tunesi, B. Correia, R. Sadeghi, E. Ghillino, P. Bardella, A. Carena, and V. Curri, "Networking analysis of photonics integrated multiband WSS based ROADM architecture," in *Proc. Int. Conf. Softw., Telecommun. Comput. Netw. (SoftCOM)*, Sep. 2022, pp. 1–6.
- [15] Y. Ma, L. Stewart, J. Armstrong, I. G. Clarke, and G. Baxter, "Recent progress of wavelength selective switch," *J. Lightw. Technol.*, vol. 39, no. 4, pp. 896–903, Feb. 2021.
- [16] *CPLEX 11.0 User's Manual.*, AMPL Optim. Inc., Mountain View, CA, USA, 2007.
- [17] M. R. Garey and D. S. Johnson, *Computers and Intractability: A Guide To the Theory of NP-Completeness*. New York, NY, USA: W. H. Freeman, 1990.
- [18] M. Klinkowski, M. Zotkiewicz, K. Walkowiak, M. Pióro, M. Ruiz, and L. Velasco, "Solving large instances of the RSA problem in flexgrid elastic optical networks," *J. Opt. Commun. Netw.*, vol. 8, no. 5, pp. 320–330, May 2016.
- [19] S. Kozdrowski, M. Zotkiewicz, and S. Sujecki, "Optimization of optical networks based on CDC-ROADM technology," *Appl. Sci.*, vol. 9, no. 3, p. 399, Jan. 2019. [Online]. Available: <http://www.mdpi.com/2076-3417/9/3/399>
- [20] M. Zotkiewicz, M. Ruiz, M. Klinkowski, M. Pióro, and L. Velasco, "Reoptimization of dynamic flexgrid optical networks after link failure repairs," *J. Opt. Commun. Netw.*, vol. 7, no. 1, pp. 49–61, Jan. 2015.
- [21] M. Dallaglio, A. Giorgetti, N. Sambo, L. Velasco, and P. Castoldi, "Routing, spectrum, and transponder assignment in elastic optical networks," *J. Lightw. Technol.*, vol. 33, no. 22, pp. 4648–4658, Nov. 2015.
- [22] S. Kozdrowski, M. Zotkiewicz, and S. Sujecki, "Ultra-wideband WDM optical network optimization," *Photonics*, vol. 7, no. 1, p. 16, Jan. 2020. [Online]. Available: <https://www.mdpi.com/2304-6732/7/1/16>
- [23] B. Shariati, A. Mastropaolo, N.-P. Diamantopoulos, J. M. Rivas-Moscoco, D. Klondis, and I. Tomkos, "Physical-layer-aware performance evaluation of SDM networks based on SMF bundles, MCFs, and FMFs," *J. Opt. Commun. Netw.*, vol. 10, no. 9, pp. 712–722, Sep. 2018.
- [24] P. Poggiolini, G. Bosco, A. Carena, V. Curri, Y. Jiang, and F. Forghieri, "The GN-model of fiber non-linear propagation and its applications," *J. Lightw. Technol.*, vol. 32, no. 4, pp. 694–721, Feb. 2014.
- [25] F. J. Moreno-Muro, R. Rumipamba-Zambrano, J. Perelló, P. Pavón-Mariño, J. Solé-Pareta, R. Martínez, R. Casellas, R. Vilalta, R. Muñoz, J. Mata, L. Ruiz, N. Merayo, I. de Miguel, and R. J. Durán, "Elastic networks thematic network results I: Planning and control of flex-grid/SDM," in *Proc. 20th Int. Conf. Transparent Opt. Netw. (ICTON)*, Jul. 2018, pp. 1–4.
- [26] R. Basir, I. Baseer, A. Ejaz, R. Ahmad, A. Baseer, A. Minhas, and J. Zahra, "Bandwidth optimization using flex grid over conventional grid for 5G optical networks," in *Proc. Int. Symp. Recent Adv. Elect. Eng. (RAEE)*, Aug. 2019, pp. 1–6.
- [27] Dostęp Zdalny. (Jun. 9, 2021). *Strona Główna Ibm Cplex Optimizer*. [Online]. Available: <https://www.ibm.com/pl-pl/analytics/cplex-optimizer>
- [28] R. Fourer, D. M. Gay, and B. W. Kernighan, "Ampl: A mathematical programming language," in *Algorithms and Model Formulations in Mathematical Programming*, S. W. Wallace Ed., Berlin, Germany: Springer, 1989, pp. 150–151.
- [29] R. Fourer, D. M. Gay, and B. W. Kernighan, "A modeling language for mathematical programming," *Manage. Sci.*, vol. 36, no. 5, pp. 519–554, May 1990. [Online]. Available: <http://www.jstor.org/stable/2632268>
- [30] S. Orłowski, R. Wessälly, M. Pióro, and A. Tomaszewski, "SNDlib 1.0—Survivable network design library," *Networks*, vol. 55, no. 3, pp. 276–286, May 2010. [Online]. Available: <https://onlinelibrary.wiley.com/doi/abs/10.1002/net.20371>
- [31] S. L. Hakimi, "On realizability of a set of integers as degrees of the vertices of a linear graph. I," *J. Soc. Ind. Appl. Math.*, vol. 10, no. 3, pp. 496–506, Sep. 1962.
- [32] M. Bayati, J. H. Kim, and A. Saberi, "A sequential algorithm for generating random graphs," *Algorithmica*, vol. 58, no. 4, pp. 860–910, Dec. 2010.



STANISŁAW KOZDROWSKI received the Ph.D. degree in technical sciences from Warsaw University of Technology, in 2000.

He is currently an Assistant Professor with the Institute of Computer Science, Faculty of Electronics and Information Technology, Warsaw University of Technology. Before defending his doctorate, he participated in a one-year internship with Lund University, Sweden. He then started working for T-Mobile Poland. He has led and participated in many projects concerning the design and optimization of optical networks. His research interests include the optimization of network problems using a variety of algorithms, in particular, nature-inspired metaheuristics. In addition, he is involved in research and development and commercial projects. These mainly concern the application of artificial intelligence in the IoT networks or machine learning algorithms in realistic next-generation optical networks. He cooperates with leading telecommunications network operator companies. He has authored and co-authored more than 50 publications in international journals and conference proceedings.



PAWEŁ KRYSZTOFIK was born in Warsaw, Poland, in 1997. He received the B.S. and M.S. degrees in information technology from Warsaw University of Technology, in 2023.

Since 2023, he has been a Junior Member of the Research and Teaching Staff with the Information Technology Department, Warsaw University of Technology. He authored so far two research articles. His research interests include optimization, metaheuristics, machine learning, and databases.



SŁAWOMIR SUJECKI (Senior Member, IEEE) received the Ph.D. and D.Sc. degrees from Warsaw University of Technology, in 1997 and 2010, respectively. He joined the University of Nottingham, in 2000, and was appointed as a Lecturer and an Associate Professor, in 2002 and 2012, respectively. Currently, he is with Wrocław University of Science and Technology and the Military University of Technology, Poland. His research interests include the design and modeling

of photonic devices and telecom networks. He is a Life Member of OSA, a member of the Program Committee of NUSOD Conference, and an Associate Editor of *Optical and Quantum Electronics*.

...